Journal of Photochemistry and Photobiology A: Chemistry 207 (2009) 224–230

Contents lists available at ScienceDirect

Journal of Photochemistry and Photobiology A: Chemistry

journal homepage: www.elsevier.com/locate/jphotochem

High efficiency quasi-solid-state dye-sensitized solar cell based on polyvinyidene fluoride-*co*-hexafluoro propylene containing propylene carbonate and acetonitrile as plasticizers

Kun-Mu Lee [a], Vembu Suryanarayanan [b], Kuo-Chuan Ho [c,*]

[a] *Photovoltaics Technology Center, Industrial Technology Research Institute, Chutung, Hsinchu 31040, Taiwan*
[b] *Electro organic Division, Central Electrochemical Research Institute, Karaikudi 630006, India*
[c] *Department of Chemical Engineering, National Taiwan University, Taipei 10617, Taiwan*

ARTICLE INFO

Article history:
Received 14 January 2009
Received in revised form 15 May 2009
Accepted 16 July 2009
Available online 24 July 2009

Keywords:
Dye-sensitized solar cell
Gel polymer electrolyte
TiO_2 morphology
Organic iodide
Electrochemical impedance spectroscopic

ABSTRACT

Quasi-solid-state dye-sensitized solar cells (DSSCs) with different weight ratios of polyvinyidene fluoride-*co*-hexafluoro propylene (PVDF-HFP) containing two different plasticizers such as propylene carbonate (PC) and acetonitrile (AN) were fabricated and the effects of TiO_2 morphology, light intensities as well as different organic iodides on the solar cell performance were studied. Two TiO_2 photoelectrodes were designed by the coating of low (P1) and high molecular weight poly(ethylene glycol) (P2) incorporated into the TiO_2 suspension. The DSSCs fabricated with the P2 TiO_2 electrode show better performance in terms of short-circuit current densities (J_{SC}) and conversion efficiencies than the P1 for all the weight percentages of PVDF-HFP containing both plasticizers. Further, the maximum current density (J_{SC}) and conversion efficiency of PVDF-HFP containing different organic iodides follow the order: TBAI > TPAI > NH_4I irrespective of the solvents and light intensity. A good conversion efficiency of 6.74% with J_{SC} of 16.04 mA/cm^2, an open-circuit voltage (V_{OC}) of 0.657 V and a fill factor of 0.64 under illumination of 100 mW/cm^2 was obtained for the DSSC with 10% of PVDF-HFP containing 0.4 M of TBAI and 0.04 M of I_2 in PVDF-HFP/AN system.

1. Introduction

Photoelectrochemical solar cells based on nanostructured dye-sensitized titanium dioxide have attracted great interest in the scientific community as a low cost alternative to the convention silicon solar cells [1,2]. A recent review work presenting an extensive listing of the highest independently confirmed efficiencies for solar cells and modules quotes that an impressive solar to electrical energy conversion efficiency of 11% can be achieved by using these types of solar cells [3]. The electrolyte used in the cell is composed of I^-/I_3^- redox couple dissolved in organic solvents [4]. However, liquid electrolytes can lead to major technological problems associated with performance limitation in long-term operation due to sealing difficulties. Hence, in order to improve the long-term stability, several kinds of strategies have been attempted to replace the liquid electrolytes by solid-state conductors such as p-type inorganic semiconductors [5] or with solid-state hole conductors [6,7]. However, the imperfect contact between the dye anchored electrode and the hole conductor in the above systems leads to inefficient hole transport resulting in the low efficiency.

In order to overcome the above problem, few alternative research works have been explored recently employing solid polymer electrolytes (SPEs). These SPEs have emerged as an exciting class of novel polymer materials with potential applications in electrochromic windows, rechargeable batteries and other devices [8]. They offer many advantages such as fast ion transport, plasticity, electrochemical stability and the ease of fabricating thin films. In one such class of polymer electrolytes, widely known as "gel polymer electrolytes", high conductivities are obtained by trapping a liquid electrolyte solution in polymer cages formed by the host matrix. Owing to their unique hybrid network structure, gels have both the cohesive properties of solids and diffusive transport of liquids and they have been characterized by high ambient ionic conductivity and long-term durability on the devices.

It is well-known that the ionic conductivity of polymer electrolytes can be enhanced using plasticizers. A plasticizer can be defined as a chemical which reduces the stiffness of an amorphous polymer. It can interact with the polymer chains on the molecular level so as to speed up the viscoelastic response of the polymer and increase the ionic mobility in the electrolyte significantly.

The first attempt to use gel electrolytes in quasi-solid-state dye-sensitized solar cells (DSSCs) was done by Cao et

* Corresponding author. Tel.: +886 2 2366 0739; fax: +886 2 2362 3040.
E-mail address: d93549007@ntu.edu.tw (K.-C. Ho).

1010-6030/$ – see front matter © 2009 Elsevier B.V. All rights reserved.
doi:10.1016/j.jphotochem.2009.07.014

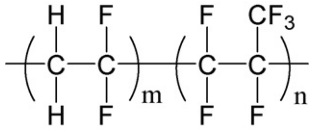

Scheme 1. The chemical structure of PVDF-HFP.

al. using poly(acrylonitrile) dissolved in ethylene carbonate/propylene carbonate/acetonitrile with specific concentration of NaI [9]. After this, there are lot of reports in the literature on the quasi-solid-state photoelectrochemical solar cells constructed with various gel electrolytes such as poly(acrylonitrile) [10–14], poly(ethyleneoxide) [15–17], poly(oligoethyleneglycol methacrylate) [18], poly(siloxane-*co*-ethylene oxide) [19], poly(butylacrylate) [20] and polyvinyidene fluoride-*co*-hexafluoro propylene (PVDF-HFP) [21–25] with different plasticizers. Among the various gel electrolytes mentioned above, PVDF-HFP (Scheme 1), shows relatively high ionic conductivities at ambient temperatures and it has been successfully used as the quasi-solid-state materials in combination with room temperature ionic liquids [23–25] showing good conversion efficiencies. Further, fluorinated polymers are potentially stable even in the presence of TiO_2 and Pt nanoparticles, which underline their suitability as a quasi-solid electrolyte in terms of long-term stability of the DSSCs [26–27]. Hence, at first, performances of the DSSC fabricated with PVDF-HFP containing PC and AN as the plasticizers having TiO_2 photoelectrodes prepared under two different conditions were investigated in this work. Further, the influence of different light intensities at different weight percentages of PVDF-HFP on the photovoltaic behavior was characterized. Finally, the effect of different cations on the redox behavior of I^-/I_3^- was also studied.

2. Experimental details

2.1. Materials

Anhydrous LiI, I_2, poly(ethylene glycol) (PEG) and 4-tertiary butyl pyridine (TBP), acetonitrile (AN), propylene carbonate (PC) and tertiary butanol were obtained from Merck. Tetrabutylammonium iodide (TBAI, +98%), tetrapropylammonium iodide (TPAI, +98%) and titanium (IV) isopropoxide (+98%) were from Acros and used as such. Ammonium iodide (NH_4I) and PVDF-HFP (molecular weight = 400,000) were obtained from Aldrich. The cis-di(thiocyanato)bis(2,2′-bipyridyl-4,4′-dicarboxylate)ruthenium (II) (N3) was obtained from Solaronix, (Aubonne, Switzerland).

2.2. Preparation of the TiO_2 electrode

The TiO_2 electrodes were prepared by sol–gel process in acid medium according to the procedure reported in the literature [4,28]. Titanium (IV) isopropoxide (72 ml, 98%, Acros) was added to 430 ml of 0.1 M nitric acid solution with constant stirring and the colloidal solution was heated to 85 °C simultaneously for 8 h. The mixture was cooled down to room temperature and filtered. Then the filtrate was heated in an autoclave at 240 °C for 12 h in order to allow the TiO_2 particles to grow uniformly. The solution was concentrated to 13 wt% and two types of pastes namely P1 and P2 were prepared by adding 30 wt% (with respect to TiO_2) of PEG with the corresponding molecular weights of 20,000 and 200,000, respectively to the above solution in order to control the pore diameters and to prevent the film from cracking during drying.

These two TiO_2 pastes (P1 and P2) were coated on a fluorine-doped tin oxide (FTO) glass plate using glass rod (the sheet resistivity of FTO is 8 Ω/square). After this, these TiO_2 photoelectrodes were dried in the air at room temperature for 30 min followed by sintering at 500 °C in a hot-oven at a rate of 5 °C/min for another 30 min. An active area of 0.25 cm^2 was selected from sintered electrode and the electrodes were immersed in 3×10^{-4} M solution of N3 dye containing acetonitrile and tertiary butanol (volume ratio of 1:1) for 24 h. Pt (100 nm thick) sputtered on FTO was used as the counter electrode.

2.3. Preparation of PVDF-HFP gel electrolytes and cell assembly

The supporting electrolyte was prepared as follows: the required weight percentage of PVDF-HFP along with I_2 (0.05 M), (0.5 M of XI, where X = NH_4^+, TBA^+, and TPA^+) were dissolved in either AN or PC and stirred at 70 °C for 6 h. When the electrolyte was cooled down, it became gel and was used as such. For measuring long-term stability, the cell was fabricated by keeping an ionomer resin (thickness of 50 μm, Dupont, USA) between the two electrodes and two holes were made on the resin. The whole set-up was heated at 100 °C on a hot plate till all the resin had been melted and the electrolyte was injected into the space between the electrodes through these two holes. Finally, these two holes were sealed completely by the Torr Seal® cement (Varian, MA, USA). For other measurements, the gel electrolyte was heated at 70 °C and immediately, it was sprayed onto the dyed TiO_2 electrode followed by clipping it with Pt electrode.

2.4. Photovoltaic measurements

The TiO_2 film thickness was measured using a profilometer (Sloan Dektak 3030). The TiO_2 surface area, pore diameter, pore volume, and particle diameter were measured by Brunauer–Emmett–Teller (BET) method, using accelerated surface area and porosimetry (Micrometrics Instruments ASAP 2010). The photoelectrochemical characterizations of the DSSCs were carried out by using an AM 1.5 simulated light radiation. The light source was a 450 W Xe lamp (#6266, Oriel) equipped with a water-based IR filter and AM 1.5G filter (#81075, Oriel).

Conductivity measurement of solution was performed by impedance spectroscopy with two Pt electrodes conductance cell where the area of the each Pt electrode is 1 cm^2 and the distance between the two electrodes is 1 cm. The cell constant is 0.54 as calibrated from the standard aqueous KCl solution. Photoelectrochemical characteristics and the electrochemical impedance spectra measurements of the DSSCs were recorded with a potentiostat/galvanostat (PGSTAT 30, Autolab, Eco-Chemie, the Netherlands) under different light illuminations. The frequency range explored was from 10 mHz to 65 kHz. The applied bias voltage and ac amplitude were set at open-circuit voltage of the DSSCs and 10 mV between the FTO/Pt counter electrode and the FTO/TiO_2/dye working electrode, respectively [29]. The impedance spectra were analyzed by an equivalent circuit model interpreting the characteristics of the DSSCs [25,30]. The structural nature of TiO_2 was investigated using Scanning Electron Microscopy (SEM, Hitachi S-4700).

3. Results and discussions

3.1. Photovoltaic studies of the DSSC

3.1.1. The influence of TiO_2 morphology on DSSC

Micrographs of the TiO_2 electrodes with the corresponding coating material of P1 and P2 obtained from SEM were shown in Fig. 1a and b respectively. Highly porous nanostructure could be observed for both the thin films from the SEM micrographs. However, it is also observed that the TiO_2 electrode coated with P2 shows high porosity and P1 shows denser structure. Further analysis of various parameters such as surface area, pore volume and pore diameter

Table 1
The specific surface area, pore diameter, pore volume of P1 and P2 TiO_2 electrodes, and the average diameter of TiO_2 particle obtained from BET measurement and SEM micrograph.

Sample	Surface area (m^2/g)	Pore diameter (nm)	Pore volume (cm^3/g)	d_{BET}[a] (nm)	d_{SEM}[a] (nm)
P1	80.4	11.5	0.29	19.2	20
P2	67.1	18.9	0.38		

[a] The diameter of TiO_2 nanoparticle.

obtained from the BET measurement of these two TiO_2 electrodes confirms the findings obtained on SEM morphology. Meanwhile, the average pore diameter of P1 was lower than that of P2 and the pore diameter distribution of P1 was narrower than P2 (Table 1). The surface area and the pore diameter of P1 were found out to be 80.4 m^2/g and 11.5 nm and P2 to be 67.1 m^2/g and 18.9 nm, respectively. Since the coating of these TiO_2 nanoparticles had been carried out under identical conditions, the diameter of the nanoparticles obtained from the SEM micrograph and BET measurements were noted as almost the same (*ca.* 20 nm). These results indicate that the morphology of the TiO_2 electrodes depends strongly on the composition and the addition of the PEG.

Fig. 2 shows the *J–V* curves of the DSSC with PVDF-HFP in PC (5 wt%) and AN (10 wt%) fabricated with P1 and P2 electrode respectively recorded under the illumination of 10 mW/cm^2. In the case of AN, a higher wt% of PVDF-HFP was needed for the process of gelification. The photovoltaic properties derived from Fig. 2 are summarized in Table 2, which also includes the data for 7 wt% and 9 wt% of PVDF-HFP in PC. DSSCs fabricated with P2 electrode

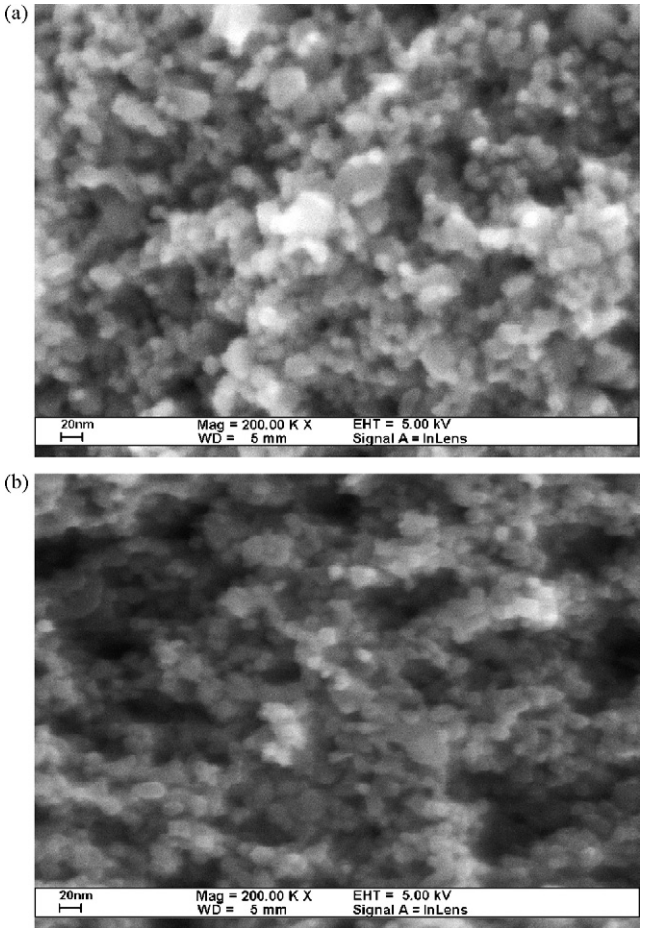

Fig. 1. The SEM images showing the surface morphologies of (a) P1 and (b) P2 TiO_2 electrodes, where P1 and P2 contain PEG binder with molecular weights of 20,000 and 200,000, respectively in the TiO_2 paste.

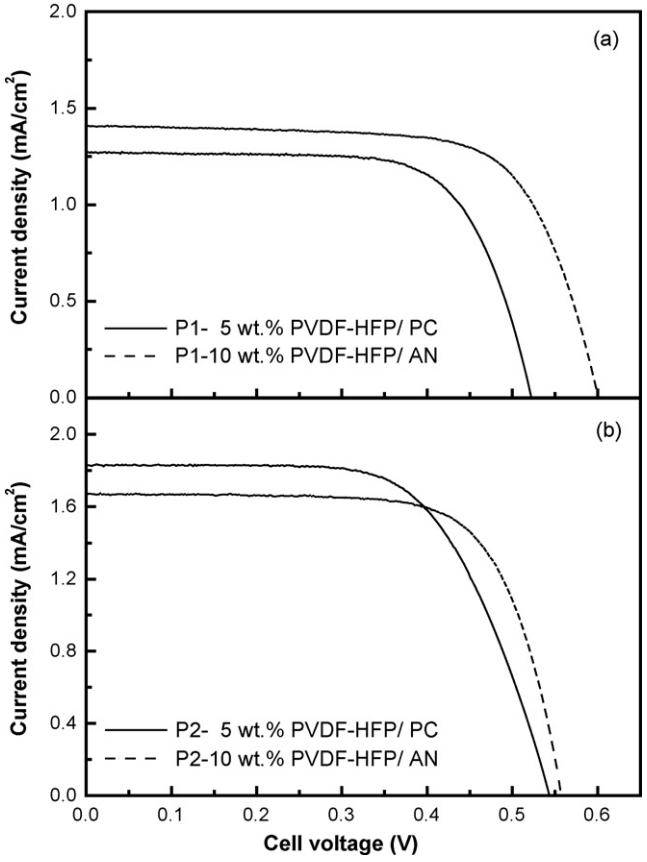

Fig. 2. Effect of TiO_2 surface morphology on the performance of the DSSC fabricated with PVDF-HFP containing PC and AN: (a) with P1 TiO_2 electrode and (b) with P2 TiO_2 electrode which measured under illumination of 10 mW/cm^2.

show better short-circuit current densities (J_{SC}) and conversion efficiencies than P1 for all the wt% of PVDF-HFP in both plasticizers (Table 2). This behavior is due to the presence of large pores in the electrode materials coated with P2, which may allow the diffusion of more redox species inside the pores. In the previous study [31], Shen and Toyoda had reported the optical absorption and electron transport properties of the TiO_2 particles having different

Table 2
The effect of TiO_2 surface morphology on the photovoltaic performance of the DSSCs with different wt% of PVDF-HFP containing PC and 10 wt% of PVDF-HFP in AN at illumination of 10 mW/cm^2.

Solvent	Weight of PVDF-HFP	Nature of TiO_2	V_{OC} (V)	J_{SC} (mA/cm^2)	η (%)	FF
PC	5%	P1	0.52	1.27	4.63	0.69
		P2	0.54	1.83	6.35	0.64
	7%	P1	0.56	1.16	4.51	0.69
		P2	0.53	1.70	5.95	0.66
	9%	P1	0.57	1.14	4.58	0.70
		P2	0.53	1.62	5.61	0.65
AN	10%	P1	0.60	1.41	5.91	0.70
		P2	0.56	1.67	6.61	0.71

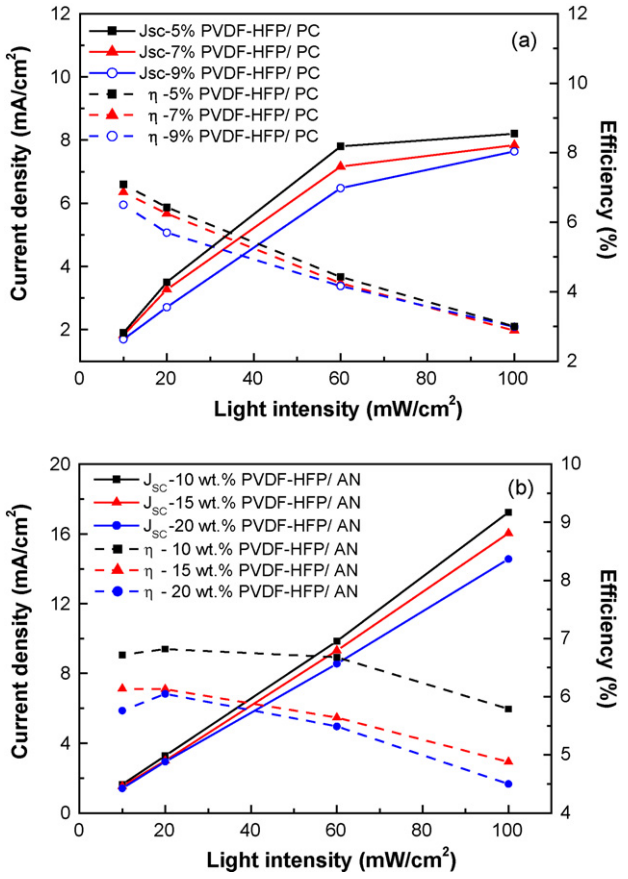

Fig. 3. Dependence of J_{SC}, V_{OC}, FF and η of the DSSC on different light intensities and various PVDF-HFP content: (a and b) for PVDF-HFP in PC and (c and d) for PVDF-HFP in AN.

pore diameters and proposed that the use of small TiO_2 particles and large pore size led to the good electron transport and high current efficiency. However, if the pore diameter is too large, the surface area of the TiO_2 particle will decrease, resulting in the poor adsorption of the dye molecule. The J_{SC} and η decrease slightly with increase in the PVDF-HFP content for the DSSC fabricated with the same P2 electrode, and the DSSC fabricated with PVDF-HFP (10 wt%) containing AN shows better photovoltaic performance than PC. The reason for this characteristic behavior will be discussed in details in the next section. A similar trend was also noticed for 15 wt% and 20 wt% of PVDF-HFP in AN where the DSSC with P2 TiO_2 electrode shows better performance (V_{OC} of 0.56 V, J_{SC} of 1.61 mA/cm^2 with η of 6.61%) than P1 TiO_2. Hence, in subsequent studies, P2 TiO_2 would be taken as the anode of choice in the DSSC.

3.1.2. *The influence of different light intensities*

The effect of different light intensities on the photovoltaic performance of the DSSC with different PVDF-HFP contents containing PC and AN was investigated. Fig. 3a and b shows the plots of different photoelectrochemical characteristics obtained for different wt% of PVDF-HFP containing PC and Fig. 3c and d shows the similar plots in PVDF-HFP containing AN. From the figures, it is observed that a linear increase of J_{SC} of the DSSC with both increase in different wt% of PVDF-HFP and the light intensities was noted in AN, whereas in PC, the increase is found to be non-linear (compare Fig. 3a and b). The linearity reveals that the light intensity-dependent photocurrent is not limited by the diffusion of I^-/I_3^- in the polymer containing AN.

Further, with increase in polymer content of DSSC, a decrease in their J_{SC} and η was noted for 10 and 100 mW/cm^2 (Fig. 3a and b) and this is more pronounced at 100 mW/cm^2. This phenomenon

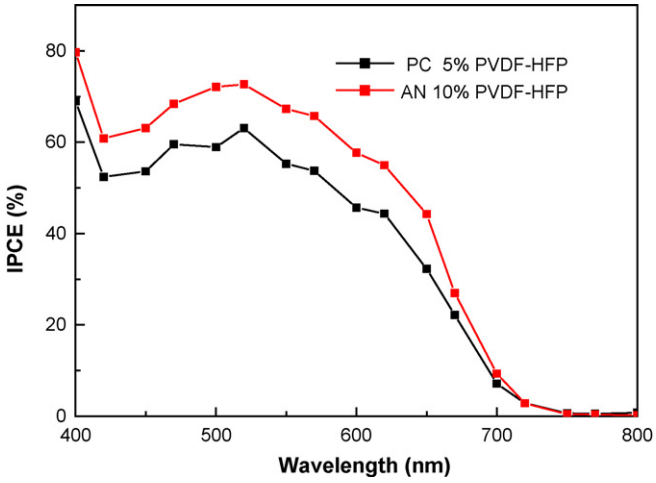

Fig. 4. IPCE of the DSSCs with PVDF-HFP containing PC and AN, respectively.

may be correlated with the ionic mobility as well as the diffusion of I^-/I_3^-. Ionic conductivity (σ) of the polymer electrolyte can be written as

$$\sigma = ne\mu \quad (1)$$

where n denotes carrier concentration, e is the charge and μ is ionic mobility [32]. The increase in the polymer content increases the viscosity of the gel electrolytes which decreases the ionic mobility, which slows down the supply of I_3^- to the Pt counter electrode causing a depletion of I_3^- at the electrode surface and this decreases the J_{SC} of the DSSC [25].

Nevertheless, the DSSC with PVDF-HFP containing AN shows better photovoltaic performance than PC. This was also reflected in IPCE (incident photon-to-current conversion efficiency) measurement of the DSSC with 5 wt% and 10 wt% PVDF-HFP containing PC and AN respectively. From Fig. 4, it is noted that the IPCE is higher in AN than in PC. The reason for this enhanced performance of AN over PC can be followed successfully from the conductivity data obtained in the form of a bar graph for different wt% of PVDF-HFP containing PC and AN in a conductivity cell which also includes the data acquired for liquid electrolyte containing TBAI/I_2 in the two solvents (Fig. 5). A three fold enhancement in the conductivity is noted if we replace PC by AN (Fig. 5) and the conductivity of

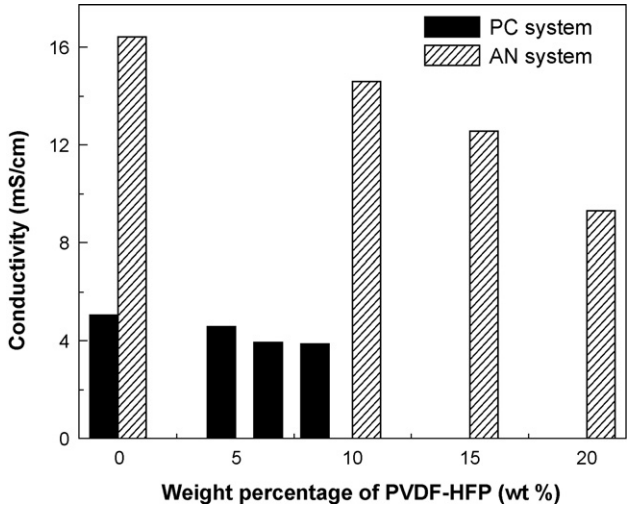

Fig. 5. Dependence of different wt% of PVDF-HFP containing PC and AN on conductivity. For comparison, liquid electrolytes containing TBAI in PC and AN are also included.

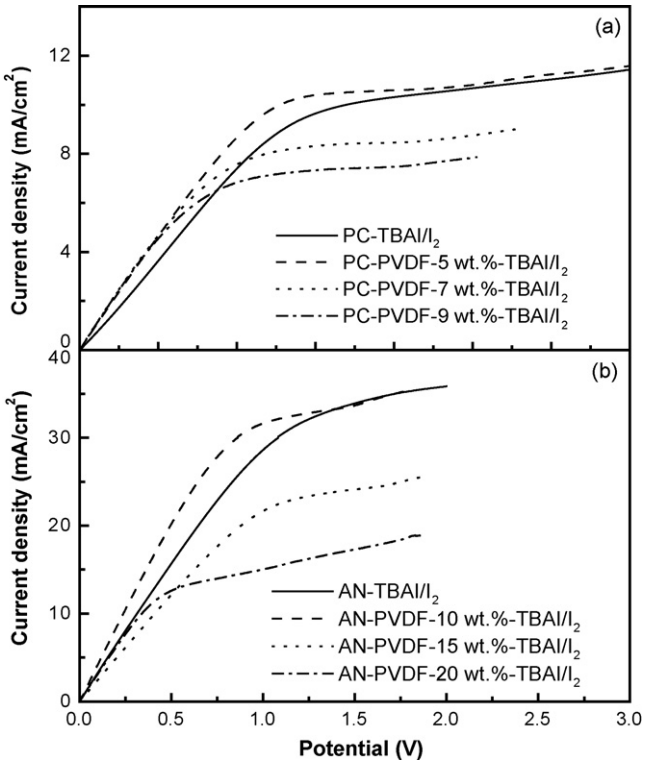

Fig. 6. Linear sweep voltammograms of cell fabricated with two Pt electrodes with different wt% of PVDF-HFP containing: (a) PC and (b) AN. For comparison, liquid electrolytes containing TBAI in (a) PC and (b) AN are also included.

10 wt% PVDF-HFP containing AN was also well comparable with the corresponding liquid electrolyte system containing TBAI/I_2. Moreover, the conductivity changes for the different wt% of PVDF-HFP are found to be minima in PC when compared to AN.

Further support for this behavior can also be obtained from the electrochemical studies of polymer electrolyte in PC and AN. Limiting current studies were carried out on a cell fabricated with two similar Pt electrodes in which the different wt% PVDF-HFP electrolyte containing PC and AN were sandwiched between them. Typical linear sweep voltammograms (LSVs) of the cells with Pt electrodes and PVDF-HFP containing PC and AN are shown in Fig. 6a and b, respectively. For comparative studies, LSVs of liquid electrolyte containing TBAI/I_2 in PC and AN were also included in the figure. From the LSVs, the diffusion coefficient, D_{app} for the AN/PVDF-HFP (10%) and PC/PVDF-HFP (5%) was calculated as ca. 6.2×10^{-6} cm^2/s and 2.3×10^{-6} cm^2/s, respectively. From this study, it is inferred that the diffusion limiting current density is also proportional to the diffusion coefficient of I^-, D_{app} [33]. The higher current density noted for AN system further supports the previous experiment and the conclusion drawn on AN based PVDF-HFP system.

It is known that various factors such as viscosity, dielectric constant and donor number of solvents show the influence on the redox properties of I^-/I_3^- couple [34]. AN has very low viscosity when compared to PC (viscosity for AN is 0.37 cp and 2.52 cp for PC); however, dielectric constant for PC is almost two times higher than AN (dielectric constant for PC and AN are 64.4 and 38) [35]. In this case, predominance of viscosity over dielectric constant is noted, which determines the ionic mobility (according to Eq. (1)) leading to the higher current density for AN/PVDF-HFP based system though both the plasticizers almost have the same donor number [37].

The back donation or recombination of electrons is a well-known process in the DSSC. In an open-circuit condition, the concentration of I_3^- is expected to be constant over the entire distance between the TiO_2 and Pt counter electrodes irrespective of the diffusion coefficient of I_3^-. Hence, the V_{OC} is independent of the diffusion coefficient of I_3^- [25]. Further, V_{OC}, a difference between Fermi level of TiO_2 and redox potential of electrolyte, is influenced mainly by the molar ratio of I^-/I_3^-, and since in our study, I^-/I_3^- molar ratio is kept constant, there are no apparent differences in the V_{OC} of the DSSC with different wt% of PVDF-HFP [32].

Table 3
Dependence of photovoltaic performance of the DSSC with 7 wt% and 15 wt% of PVDF-HFP in PC and AN, respectively, on different organic iodides under two different light intensities of 10 and 100 mW/cm^2.

Light intensity (mW/cm^2)	Solvent	Iodides	J_{SC} (mA/cm^2)	V_{OC} (V)	η (%)	FF
10	PC	TBAI	1.46	0.531	5.45	0.70
		TPAI	1.26	0.571	4.78	0.67
		NH_4I	1.07	0.507	3.49	0.64
	AN	TBAI	1.53	0.571	6.14	0.70
		TPAI	1.00	0.531	4.28	0.69
		NH_4I	0.68	0.433	1.82	0.62
100	PC	TBAI	7.84	0.670	3.57	0.68
		TPAI	7.56	0.659	3.19	0.64
		NH_4I	4.32	0.605	1.83	0.70
	AN	TBAI	16.04	0.657	6.74	0.64
		TPAI	12.88	0.627	5.33	0.66
		NH_4I	6.40	0.523	2.34	0.70

3.1.3. The influence of different organic iodides

Three different organic iodides such as tetrabutylammonium (TBAI), tetrapropylammonium (TPAI) and ammonium iodide (NH_4I) have been selected and the photoelectrochemical characteristics of 7 wt% and 15 wt% PVDF-HFP in PC and AN, respectively, containing the above organic iodides have been studied. Table 4 shows the data for the light intensities of 10 and 100 mW/cm^2. The maximum J_{SC} and conversion efficiency of the DSSC based on PVDF-HFP containing the organic iodides follows the order TBAI > TPAI > NH_4I irrespective of the solvents and light intensities. The reason for higher J_{SC} in case of PVDF-HFP system containing TBAI may be associated with increase in the conduction band level of the TiO_2 positively, which can enhance the energy gap and the driving force for the electron injection process between the LUMO level of the dye and the conduction band of the TiO_2 [36]. Moreover, PVDF-HFP containing NH_4I exhibits very low V_{OC} under all the above conditions when compared to the other organic iodides (Table 3) and this can be correlated with two reasons: one is with small energy gap between conduction band of the TiO_2 and the redox potential of iodide in NH_4^+ cation [36] and second is lesser solubility of NH_4I in AN and PC when compared to other cations.

In case of PC as the plasticizer, the efficiency decreases almost 40% in enhancing the light intensities from 10 to 100 mW/cm^2 (Table 3); however, the performance was almost the same in AN system and once again, the PVDF-HFP containing AN shows better performance than PC under the both light intensities of 10 and 100 mW/cm^2.

3.2. Electrochemical impedance spectroscopic (EIS) studies of the DSSC

Fig. 7 shows the EIS analysis for the DSSC with different wt% of PVDF-HFP containing PC and AN respectively. All the spectra exhibit three semicircles (A, B and C), which are assigned to electrochemical reaction at Pt electrode interface, TiO_2/dye/electrolyte interface and Warburg diffusion process of I_3^- in electrolyte [29,30]. The equivalent circuit employed for the curve fitting of the impedance spectra of the DSSCs is shown in Fig. 7c, and the parameters obtained by fitting of the impedance spectra of the DSSCs are also summarized in Table 4. The symbol R_s represents the series resistance com-

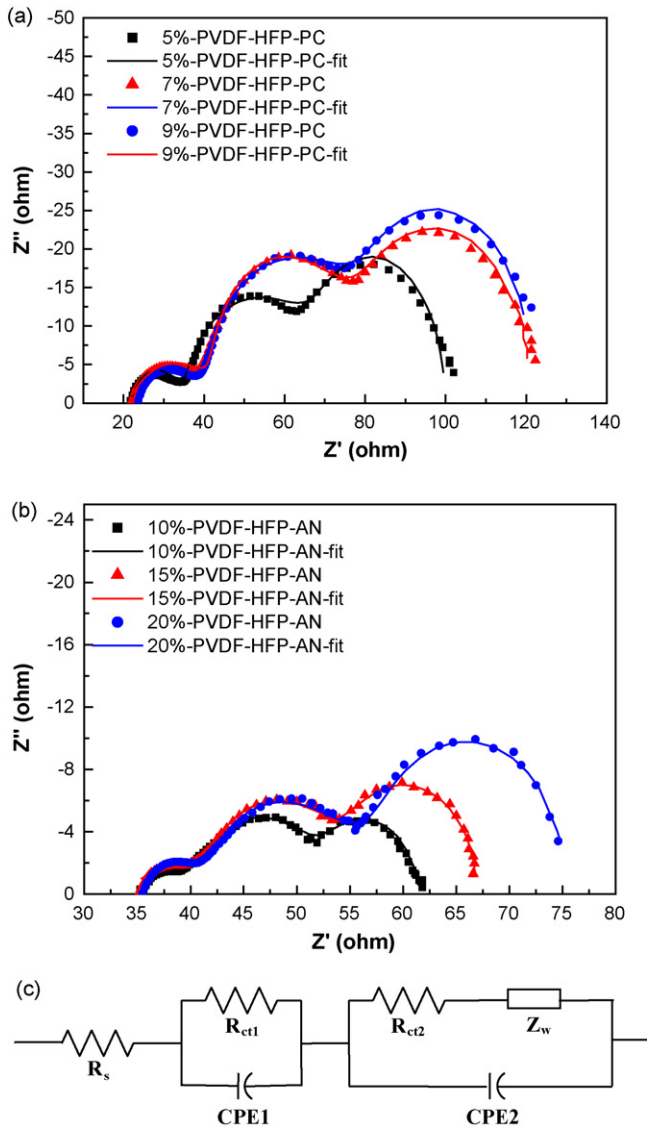

Fig. 7. EIS of the DSSC with different wt% of PVDF-HFP electrolyte containing (a) PC and (b) AN. (c) Equivalent circuit model used for the DSSC in this study.

posed of the resistance of the electrolyte and the sheet resistance of the electrodes. The symbol R_{ct1} and R_{ct2} are the charge transfer resistances of Pt/electrolyte interface and TiO_2/dye/electrolyte interface, respectively. Z_W is the finite-length Warburg diffusion impedance and CPEi (i = 1 and 2) is the constant phase element. With the increase in the polymer content, R_{ct1} and R_{ct2} increase and this establishes a poor charge transfer between polymer film and Pt as well as TiO_2 dye interfaces (Table 4). Meanwhile, Kern et

Table 4
Impedance parameters of DSSCs with different wt% PVDF-HFP containing AN and PC.

Solvent	Weight% of PVDF-HFP	R_{ct1} (ohm)	R_{ct2} (ohm)	τ_e (ms)	R_{diff} (ohm)
AN	10	9.0	7.7	18.2	10.1
	15	9.3	9.9	17.5	14.0
	20	9.7	12.9	16.8	20.9
PC	5	12.8	28.1	16.6	35.2
	7	20.1	30.2	16.1	48.5
	9	22.3	33.1	15.7	52.5

τ_e: electron lifetime, which is calculated from the EIS data.

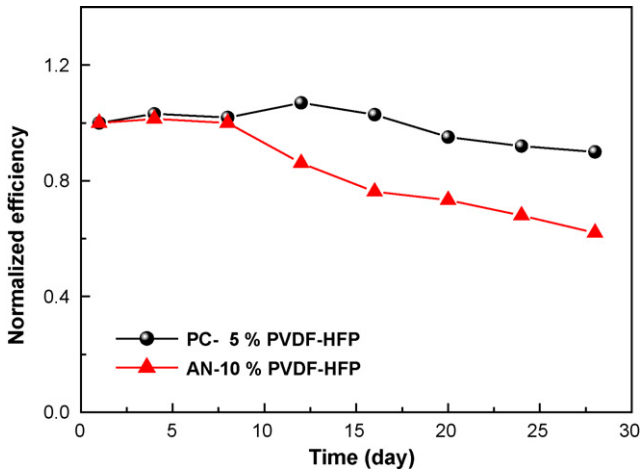

Fig. 8. Variation of energy conversion efficiency as a function of time in days for a quasi-solid DSSC with PVDF-HFP containing (a) PC and (b) AN.

al. [37] reported that the electron lifetime (τ_e) of charge transfer at TiO_2/electrolyte interface could be calculated using the characteristic frequency at the top of the semicircle (f_c) using the following equation:

$$\tau_e = \frac{1}{2}\pi f_c \quad (2)$$

It is suggested that the τ_e value estimated from EIS measurement under open-circuit condition indicated a probability of back electron transfer from the TiO_2 surface to the I_3^- in the electrolyte. The values of τ_e are also listed in Table 4 where the AN based DSSCs have higher τ_e than that of PC based system, and the τ_e decreases slightly with the increase in the polymer content. This may be correlated with the decrease in the ionic diffusion coefficient of I_3^-, leading to a decrease of J_{SC}. This reveals that the ionic mobility of the electrolyte is one of the important factors in determining the cell performance of the DSSCs. It is also noted that the DSSC containing PVDF-HFP/PC exhibits higher charge transfer resistance than that of AN. This can be correlated with their difference in dielectric constants and viscosities.

3.3. At-rest long-term stability of DSSCs

The evolution of conversion efficiencies with time in days for both the cells with PVDF-HFP containing PC and AN, respectively, are shown in Fig. 8. The DSSC containing PC as the plasticizer sustains 13% of the energy efficiency after 28 days, whereas in AN, the energy loss is slightly high (almost 3.5 times higher than the former) and this may be correlated with evaporation of solvents which is considered to be more in the DSSC containing AN than PC and this may be correlated with high boiling point of PC when compared to AN.

4. Conclusion

The effects of different photoelectrode surface morphology, light intensities and organic iodides on the photovoltaic performance of the DSSC with different wt% of PVDF-HFP containing PC and AN were studied. P2 TiO_2 photoelectrode incorporated with high molecular weight PEG shows better performance in terms of their J_{SC} and conversion efficiency for all the weight percentages of PVDF-HFP. A linear increase of J_{SC} of the DSSC with both increase in different wt% of PVDF-HFP and the light intensities was noted in AN, whereas in PC, the increase is found to be non-linear, which can be correlated with the high conductivity and low viscosity of the former solvent. The stability of energy efficiency of the DSSC

with PVDF-HFP containing PC sustains 13 % of its initial value, while in AN, the loss is slightly high. Because of the good stability and favorable conversion efficiency, PVDF-HFP has become a promising gelator for the DSSC.

Acknowledgement

This work was financially supported by the Academia Sinica, Taipei, Taiwan, the Republic of China, under grant AS-97-TP-A08.

References

[1] B. O'Reagen, M. Grätzel, A low-cost, high-efficiency solar cell based on dye-sensitized colloidal TiO_2 films, Nature 353 (1991) 737–740.
[2] A. Hagfeldt, M. Grätzel, Light-induced redox reactions in nanocrystalline systems, Chem. Rev. 95 (1995) 49–68.
[3] M.A. Green, K. Emery, Y. Hishikawa, W. Warta, Solar cell efficiency tables, Prog. Photovolt.: Res. Appl. 17 (2009) 85–94.
[4] C.J. Baede, F. Arendsc, P. Comte, M. Jirousek, F. Lenzmann, V. Sshklover, M. Grätzel, Carbocation-mediated processes in biocatalysts. Contribution of aromatic moieties, J. Am. Ceram. Soc. 80 (1997) 3157–3161.
[5] B.O. Reagan, D. Schwartz, Large enhancement in photocurrent efficiency caused by UV illumination of the dye-sensitized heterojunction TiO_2/RuLL'NCS/CuSCN: initiation and potential mechanisms, Chem. Mater. 10 (1998) 1501–1509.
[6] K. Murakoshi, R. Kogue, Y. Wada, S. Yanagida, Solid state dye-sensitized TiO_2 solar cell with polypyrrole as hole transport layer, Chem. Lett. (1997) 471–474.
[7] U. Bach, D. Lupo, P. Comte, J.E. Moser, F. Wiessortel, J. Salbeck, H. Spreitzer, M. Grätzel, Solid-state dye-sensitized mesoporous TiO_2 solar cells with high photon-to-electron conversion efficiencies, Nature 395 (1998) 583–585.
[8] C.A. Wincent, B. Scrosatti, Modern Batteries—An Introduction to Electrochemical Power Sources, Wiley, New York, 1997.
[9] F. Cao, G. Oskam, P.C. Searson, A solid state, dye sensitized photoelectrochemical cell, J. Phys. Chem. 99 (1995) 17071–17073.
[10] G. Wang, X. Zhou, M. Li, J. Zhang, J. Kang, Y. Lin, S. Fang, X. Xiao, Gel polymer electrolytes based on polyacrylonitrile and a novel quaternary ammonium salt for dye-sensitized solar cells, Mater. Res. Bull. 39 (2004) 2113–2118.
[11] M.A.K.L. Dissanayake, L.R.A.K. Bandara, R.S.P. Bokalawala, P.A.R.D. Jayathilaka, O.A. Illeperuma, S. Somasundaram, Reflective liquid-crystal displays, Mater. Res. Bull. 37 (2002) 867–872.
[12] O.A. Illeperuma, M.A.K.L. Dissanayake, S. Somasundaram, Dye-sensitised photoelectrochemical solar cells with polyacrylonitrile based solid polymer electrolytes, Electrochim. Acta 47 (2002) 2801–2807.
[13] O.A. Illeperuma, M.A.K.L. Dissanayake, S. Somasundaram, L.R.A.K. Bandara, Photoelectrochemical solar cells with polyacrylonitrile-based and polyethylene oxide-based polymer electrolytes, Sol. Energy Mater. Sol. Cells 84 (2004) 117–124.
[14] J. Kang, W. Li, X. Wang, Y. Lin, X. Li, X. Xiao, S. Fang, Gel polymer electrolytes based on a novel quaternary ammonium salt for dye-sensitized solar cells, J. Appl. Electrochem. 34 (2004) 301–304.
[15] G. Katsaros, T. Stergiopoulos, I.M. Arabatzis, K.G. Papadokostaki, P. Falaras, A solvent-free composite polymer/inorganic oxide electrolyte for high efficiency solid-state dye-sensitized solar cells, J. Photochem. Photobiol A: Chem. 149 (2002) 191–198.
[16] T. Stergiopoulos, I.M. Arabatzis, G. Katsaros, P. Falaras, Binary polyethylene oxide/titania solid-state redox electrolyte for highly efficient nanocrystalline TiO_2 photoelectrochemical cells, Nano Lett. 2 (2002) 1259–1261.
[17] Y.J. Kim, J.H. Kim, M.S. Kang, M.J. Lee, J. Won, J.C. Lee, Y.S. Kang, Supramolecular electrolytes for use in highly efficient dye-sensitized solar cells, Adv. Mater. 16 (2004) 1753–1759.
[18] M. Masamitsu, M. Hiromitsu, M. Kikuo, K. Yoshimasa, T. Yoichi, A dye sensitized TiO_2 photoelectrochemical cell constructed with polymer solid electrolyte, Solid State Ionics 89 (1996) 263–267.
[19] Y. Liu, J.Y. Lee, L. Hong, In situ preparation of poly(ethylene oxide)–SiO_2 composite polymer electrolytes, J. Power Sources 129 (2004) 303–306.
[20] J.H. Kim, M.S. Sung, Y.J. Kim, J. Won, Y.S. Kang, Poly(butyl acrylate)/NaI/I_2 electrolytes for dye-sensitized nanocrystalline TiO_2 solar cells, Solid State Ionics 176 (2005) 579–584.
[21] P. Wang, S.M. Zakeeruddin, I. Exnar, M. Grätzel, High efficiency dye-sensitized nanocrystalline solar cells based on ionic liquid polymer gel electrolyte, Chem. Commun. (2002) 2972–2973.
[22] S.R. Scully, M.T. Lloyd, R. Herrera, E.P. Giannelis, G.G. Malliaras, Dye-sensitized solar cells employing a highly conductive and mechanically robust nanocomposite gel electrolyte, Synth. Met. 144 (2001) 291–294.
[23] K.M. Lee, V. Suryanarayanan, K.C. Ho, A photo-physical and electrochemical impedance spectroscopy study on the quasi-solid state dye-sensitized solar cells based on poly(vinylidene fluoride-co-hexafluoropropylene), J. Power Sources 185 (2008) 1605–1612.
[24] P. Wang, S.M. Zakeeruddin, M. Grätzel, Solidifying liquid electrolytes with fluorine polymer and silica nanoparticles for quasi-solid dye-sensitized solar cells, J. Fluorine Chem. 125 (2004) 1241–1245.
[25] T. Asano, T. Kubo, Y. Nishikitani, Electrochemical properties of dye-sensitized solar cells fabricated with PVDF-type polymeric solid electrolytes, J. Photochem. Photobiol. A: Chem. 164 (2004) 111–115.
[26] F.R.F. Fan, H.Y. Liu, A.J. Bard, Integrated chemical systems: photocatalysis at titanium dioxide incorporated into Nafion and clay, J. Phys. Chem. 89 (1985) 4418–4420.
[27] L. Kaven, M. Grätzel, Nafion modified TiO_2 electrodes: photoresponse and sensitization by Ru(II)-bipyridyl complexes, Electrochim. Acta 34 (1989) 1327–1334.
[28] M.K. Nazeeruddin, R. Humphry-Baker, P. Liska, M. Grätzel, Investigation of sensitizer adsorption and the influence of protons on current and voltage of a dye-sensitized nanocrystalline TiO_2 solar cell, J. Phys. Chem. B 107 (2003) 8981–8987.
[29] C. Longo, J. Freitas, M.A. De Paoli, Performance and stability of TiO_2/dye solar cells assembled with flexible electrodes and a polymer electrolyte, J. Photochem. Photobiol. A: Chem. 159 (2003) 33–39.
[30] M.C. Bernard, H. Cachet, P. Falaras, A. Hugot-Le Goff, M. Kalbac, I. Lukes, N.T. Oanh, T. Stergiopoulos, I. Arabatzis, Sensitization of TiO_2 by polypyridine dyes, J. Electrochem. Soc. 150 (2003) E155–E164.
[31] Q. Shen, T. Toyoda, Studies of optical absorption and electron transport in nanocrystalline TiO_2 electrodes, Thin Solid Films 438–439 (2003) 167–170.
[32] R. Koyima, L. Han, R. Yamanaka, A. Islam, T. Mitae, Highly efficient quasi-solid state dye-sensitized solar cell with ion conducting polymer electrolyte, J. Photochem. Photobiol. A: Chem. 164 (2004) 123–127.
[33] A. Hauch, A. Grorg, Diffusion in the electrolyte and charge-transfer reaction at the platinum electrode in dye-sensitized solar cells, Electrochim. Acta 46 (2001) 3457–3466.
[34] S.S. Sekhon, N. Arora, H.P. Singh, Effect of donor number of solvent on the conductivity behaviour of nonaqueous proton-conducting polymer gel electrolytes, Solid State Ionics 160 (2003) 301–307.
[35] A. Fukui, R. Komiya, R. Yamanaka, A. Islam, L. Han, Effect of a redox electrolyte in mixed solvents on the photovoltaic performance of a dye-sensitized solar cell, Sol. Energy Mater. Sol. Cells 90 (2005) 649–658.
[36] K. Hara, T. Horiguchi, T. Kinoshita, K. Sayama, H. Arakawa, Influence of electrolytes on the photovoltaic performance of organic dye-sensitized nanocrystalline TiO_2 solar cells, Sol. Energy Mater. Sol. Cells 70 (2001) 151–161.
[37] R. Kern, R. Sastrawan, J. Ferber, R. Stangl, J. Luther, Modeling and interpretation of electric impedance spectra of dye solar cells operated under open-circuit conditions, Electrochim. Acta 47 (2002) 4213–4225.